

Spaceflight Exercise and Textile Laundering Machine for Improved Human Health

Andrew R. Arends[1] and Stephen K. Robinson[2]
University of California Davis, Davis, CA, 95616

Without a precedent to laundering clothes off-Earth, a preliminary solution space is required to develop a spaceflight laundry machine capable of operating in various gravity fields. With this paper's proposed solution space, human exercise to power a vibration agitation bladder, a closed-loop hydraulic system, and a wastewater sensor suite provide a desirable environment for quantifying waste-mass transfer away from textiles while reducing textile damage. Bond Graph Theory is used to evaluate how human power affects system and cleaning performance because it is amenable to the large variety of machine configurations humans can set and to the coupling expected within the different subsystems. Bond Graph simulation results reveal preliminary performance metrics, sensor types and placements, and the hardware significantly impacting the spaceflight exercise and textile laundering machine's performance. Last, this paper's methodology provides structure in maturing the machine's Spaceflight Technology Readiness Level beyond its current state.

Nomenclature

a_1	= Crank arm mount to plate hinge length
a_2	= Shock absorber set #1 to plate hinge length
a_3	= Shock absorber set #2 to plate hinge length
$A(u)$	= Valve area as a function of valve position
A_A	= Cross-sectional area of agitation chamber
A_p	= Cross-sectional area of hydraulic piping
A_{lcp}	= Cross-sectional area of lint catch
A_{wfp}	= Cross-sectional area of water filter
ARED	= Advanced Resistive Exercise Device
b_c	= Crank arm mount damping coefficient
b_{cs}	= Crankshaft friction
b_{sa}	= Tilt plate shock absorber damping coefficient
b_{tp}	= Tilt plate damping coefficient
B	= Bulk Modulus
BIBO	= Bounded Input Bounded Output
BG	= Bond Graph
$\bar{c}$	= Average amount of waste removed
Δc	= Concentration of waste in water
$C_d(u)$	= Valve discharge coefficient function
$D_{P_{lc}}$	= Particle diameter of lint catch
$D_{P_{wf}}$	= Particle diameter of water filter
E	= Elastic modulus of bladder rubber
ISS	= International Space Station
J_C	= Inertia of crankshaft
LED	= Light-emitting Diode
n	= Kinetic order
$\dot{p}_c$	= Net torque acting on crankshaft
$\dot{p}_{h_1}$	= Net pressure of hydraulic flow path #1
$\dot{p}_{h_2}$	= Net pressure of hydraulic flow path #2
$\dot{p}_{tp}$	= Net torque acting on tilt plate
$\dot{q}_{sa_1}$	= Axial velocity for shock absorber set #1
$\dot{q}_{sa_2}$	= Axial velocity for shock absorber set #2
$\dot{q}_{tp}$	= Rotational velocity of tilt plate
ΔQ	= Flow rate difference for BG element
r	= Crank arm mount to crankshaft center length
r_A	= Radius of agitation bladder corners
r_R	= Radius of water reservoir bladder corners
R_e	= Electrical circuit resistance
R_{lc}	= Linear lint catch resistance
R_{wf}	= Linear water filter resistance
t	= Simulation run time
t_A	= Thickness of agitation bladder
t_R	= Thickness of water reservoir bladder
T_{em}	= DC generator rate #1
T_{me}	= DC generator rate #2
T_P	= Hydraulic pump rate
u	= Hydraulic valve position as a percentage
V_A	= Volume of agitation bladder

[1]Master's Student - Mechanical and Aerospace Engineering Department, University of California Davis, One Shields Ave., Davis, CA 95616-5270, ararends@ucdavis.edu
[2]Professor, Director - UC Davis Center for Spaceflight Research, University of California Davis, One Shields Ave., Davis, CA 95616-5270, stephen.k.robinson@ucdavis.edu

$J_{tp}(q_a)$ = Inertia of tilt plate function
k = Waste removal rate coefficient
k_c = Crank arm mount stiffness coefficient
k_s = Waste removal rate scaling factor
k_{sa} = Tilt plate shock absorber stiffness coefficient
k_{tp} = Tilt plate stiffness coefficient
L_{lc} = Length of lint catch
L_{wr} = Length of water reservoir
l = Length of crank arm
l_p = Length of hydraulic pipe path
l_{tp} = Length of square tilt plate
LEO = Low Earth Orbit
V_P = Volume of piping
V_R = Volume of water reservoir bladder
V_T = Volume of textiles
V_{wf} = Volume of water filter(s)
α = Position of tilt plate rotation
ε_{lc} = Porosity of lint catch
ε_{wr} = Porosity of water reservoir
ρ = Density of washing fluid
θ = Position of crankshaft rotation
$\tau(t)$ = Human Generated torque over time
μ = Dynamic viscosity of washing fluid

I. Introduction

From language to preferred diets and workout regimens, human spaceflight programs have addressed fundamental behaviors of humans, except a frequent activity thousands of years old. Laundering textiles is inherently human and something essential to human life. Leaving Earth's gravity for prolonged periods rapidly deteriorates the human body, requiring astronauts to exercise for multiple hours during a twenty-four-hour period to avoid long-term health risks. An extended exercise period saturates textiles with perspiration, dead skin, and other bodily fluids. Exposure to human excretions for prolonged periods also poses a health risk to the human body. Without convenient or traditional medical treatments off-Earth to address health risks, future spaceflight operations must address storing saturated textiles and donning clean textiles multiple times during a twenty-four-hour period while off-Earth.

The dirty textiles go where the humans go. Off-Earth surface activities, such as showering and horizontal sleeping, will require the laundering of towels and sheets. Transit between planetary bodies will also produce contaminated textiles. From a logistical spaceflight stance, it is not practical to continually discard and resupply exercise clothing during an extended duration mission. During a 3-year mission to Mars without textile laundering, *each* crew member may go through about 210 kg (460 lbs.) of textiles, with attendant launch and transport costs.[1] In addition, future long-duration Low Earth Orbit (LEO) tourism programs will need to address textile logistics for their customers.

There is potential for a future with humans in LEO, on the Moon, and on Mars simultaneously performing a wide range of physical activities. As humans develop and improve living conditions off-Earth, our time off-Earth will increase, increasing our need for clean textiles to replace our contaminated textiles. Overall, spaceflight textiles consume volume, add mass, and require the forethought of handling and replacing once soiled. *To address the problem of soiled textiles off-Earth, an approach to laundering textiles in space vehicles and habitats may consider human exercise as power input, wastewater recycling, customizable textile agitation to remove a variety of textile contaminates, and feedback metrics for textile cleanliness while operating in a variety of gravity fields.* Section II of this paper is a Literature Review to outline laundering mechanics, textile cleanliness quantification, and spaceflight health improvement measures and design principles. Section III proposes a solution to laundering textiles off-Earth in the context of the Literature Review. Section IV outlines the Bond Graph methodology used to analyze the laundering problem, with the corresponding results reported in Section V. Lastly, a concluding discussion on the information presented in the paper and the next steps in developing the exercise and laundering machine is presented.

II. Literature Review

A. Overview

There is no precedent to laundering textiles off-Earth reliably; however, the collective human knowledge of laundering textiles has identified a few core aspects of laundering for off-Earth living. The objective of laundering clothing is to transport waste matter away from textiles. Traditional laundering combines water, heat and mechanical agitation energy, and chemicals in a complex matrix of time-dependent rate-driven relationships. Contaminants naturally diffuse out of textiles submerged in water, and more waste can be removed (dispersed) by inputting mechanical power from hydrodynamics, abrasion, and fiber flexing. The mechanical actions promote the rolling-up of oils off textiles, penetration and degradation of attached particulates, and the solubilization and emulsification of the washing fluid. After a long washing period without replacing the washing fluid, the redeposition rate of waste onto textiles is negligible; however, hard and pre-contaminated water plays a significant role in the overall laundering

efficiency regardless of water, energy, chemical, and textile combination.[2-9] Furthering the complexity of laundry, the waste-textile combination is an essential factor in the mass dynamics of laundry.

Depending on how waste enters and interacts with textiles, specific laundering configurations become more impactful. Textile wastes are either soluble, saponifiable, emulsifiable, or inert. Soluble waste readily dissolves in water, saponifiable waste contains lipids that react with alkalis to become soluble soaps, and emulsifiable waste does not react with alkalis and is often petroleum-based. Inert waste consists of abrasive particles such as lunar regolith. Waste mass enters textile matrices through textiles siphoning dirty water and textile-waste collisions. Waste is held in place by Van der Waal's forces, chemical bonds, and the location of waste relative to fabric cores (the microfibers at the center of fiber bundles). The closer the waste is to the fabric cores, the further away the waste is from the water flow path, thereby lowering the probability of waste detaching from textiles during the laundering process. In addition, if large pores are present in the textile's fabric weave, water flow increases through the textile and increases the likelihood of waste removal.

Textile material properties influence washing fluid absorption, abrasion resistance, and flexibility. Materials that swell reduce the water flow path area and the waste's overall diffusion and dispersion rate. Regardless of configuration, the rate of waste removal can be simplified and temporally generalized through a log-log relationship (see Section IV.E). Deviations from the relationship occur due to the changing laundering environment; regardless, most waste removal occurs within the first twenty minutes of laundering.[6-9] However, no work found in literature addresses how alternating gravitational fields will impact a laundering process and the end cleanliness of laundered textiles.

In a constant 1-g field, gravitational forces overcome water surface tension forces, and the free surface of resting water can be assumed to be normal to the gravity vector. Reduction of the gravity vector magnitude enables surface tension to be the dominating force acting on water.[10] Because gravitational fields generate a potential energy field for matter, calibrated systems perform suboptimally if the gravity field changes, i.e., the head acting on hydraulic reservoirs changes, the pipe fluid dynamics change, the equilibrium point of mass-spring-damper systems changes, and the loading from masses change. Similar to how mass dynamics change with changing gravity fields, biomechanics and bioprocesses in living organisms change in alternating gravity fields leading to organism atrophy.

Over extended periods of non-Earth gravity levels, simple exercise machines counter human body atrophy. The prominent degradation of human bodies in spaceflight occurs in the first four months, with the cardiovascular, musculoskeletal, and muscle systems being impacted the most by the removal of Earth's gravity.[11] Humans' legs, hips, and lower back are especially susceptible to reduction in bone tissue and muscle density, strength, and volume due to the lack of loading on the legs while off-Earth. Aerobic and resistive exercise can improve red blood cell count and skeletal structure to combat the cell atrophy that causes fiber strength and power declines. Countering atrophy is vital to promote adequate in-flight crew mission performance, safe Earth reentry, and post-flight recovery.[11-17] Due to the importance of exercise off-Earth and spaceflight resource management, exercise machines gain mechanical robustness from simple low-volume and mass designs for maintenance, usage, and vibration isolation. Frequent exercise produces liquid perspiration and other waste that contaminate and produce biohazard-ridden textiles, which is why a link from on-Earth to off-Earth laundering is needed.

This review discusses laundry agitation, textile cleanliness evaluation methods, and capturing human power in spaceflight. First, References 18 – 22 suggest high-frequency fiber flexing and clean flowing water being the best promotors of waste transfer off textiles. Next, to quantify general cleanliness during a laundering process, References 23-29 suggest observations of electrolyte, organic, and particulate waste transported away from textiles. Lastly, considerations to convert human energy to mechanical work in spaceflight are explored.[1,10-17,30-32] Together, the aforementioned References offer a novel solution space to model, design, and evaluate a spaceflight exercise and textile laundering machine to improve human health.

B. Discussion

1. Laundry Agitation Methods

Textile agitation in the laundering process is essential to remove waste with chemical and physical reactions efficiently; however, agitation methods have different waste-removing capabilities. References 18-20 evaluate and compare the four most common laundering textile agitation methods using the same cleanliness quantification method (fluorescence measurements). References 21 and 22 expand on the idea of agitating with high-frequency inputs to promote a higher rate of waste transfer. The controlled agitation methods discussed in this section conclude that rapidly pushing and pulling the fiber matrix with clean rinsing water encourages textiles to efficiently expel waste attached to the inner fiber cores.

Although Ref. 18 evaluated abrasive laundering in a controlled environment, the cleanliness results also depended heavily on the water temperature, and textile damage results were not reported, which reaffirms Ref. 19 and 20's trade

space on controlled agitation. In general, abrasive water-textile impacts and textile fiber flexing break van der Waal's forces holding particulates and promote the rolling up and release of liposoluble waste.[19] Although Ref. 19 concluded that soaking and hydrodynamics do not cause significant fiber flexing, Ref. 20 found that clean water promotes a highly favorable concentration gradient for waste transfer away from fibers comparable to hydrodynamics. Both Refs. 18 and 19 note the potential textile damage of highly abrasive laundering; however, they do not mention damage potential from high-frequency flexing of the fibers.

Unlike agitators and impellers, ultrasonic laundering controls fiber flexing; Refs. 21 and 22 agree that the asymmetrical collapse of pressure waves near the textile during ultrasonic laundering compresses and stretches the fibers. As a result, Ultrasonics promotes waste dispersion into the water, but most energy goes into deforming the textiles.[21] Ref. 22 addresses the high-frequency abrasion concerns of Ref. 21 by performing a detailed inspection of the textile's structure before and after laundering. Ref. 22 found that ultrasonic-laundered fibers had better tensile strength retention in both the warp (transverse weave) and weft (longitudinal) directions with minimal abrasive and cavitation damage compared to agitation machines. Therefore, high-frequency flexing textile fibers increase their water contact area over a longer period, increasing the area and opportunity for waste to transfer off the textile.

In summary, Refs. 18 – 22 showed that waste transfer depends on abrasion, fiber flexing, and water cleanliness. Refs. 20 – 22 expand upon Refs. 18 and 19 by concluding that high-frequency fiber flexing rapidly pushes and pulls fibers in such a way that waste transfer increases and textile damage decreases compared to other traditional mechanical agitations—however, Refs. 2-9,18-23 do not acknowledge the waste-removing ability of fiber flexing at high frequencies with a continuous clean crossflow to promote waste transfer and transport. Furthermore, the References used limited textile-waste combinations due to the cleanliness quantification method.

2. Textile Cleanliness Quantification Processes.

Different combinations of water quantity and temperature, agitation method and duration, and added detergents all impact the cleanliness of textiles; however, the quantification of textile cleanliness is not trivial. References 23 through 27 discuss reflectance, irradiation, and image analysis methods that quantify the amount of specific waste remaining on a single type of fabric or textile after laundering. To address the shortcomings of labor-intensive analysis of specific waste-textile combinations, References 21, 28, and 29 evaluate cleanliness through methods targeting waste's chemical characteristics in bulk textiles instead of single article combinations. Understanding the transfer and transport mechanics and chemical properties of waste embedded in textiles leads to observing contaminates in wastewater for textile cleanliness quantification.

Different wavelengths of photons used in spectroscopy and microscopy methods quantify how much specific waste is on a textile; Ref. 23 – 27 show how different models can be used at different wavelengths to quantify the cleanliness of a single waste-textile combination. The Kubelka–Munk equation based on reflectance (visible light microscopy) measurements is a widely used model; however, it requires the dying of textile waste and knowledge of textile-waste combinations to calibrate measurements.[18-20, 23, 26, 27]

Alternatively, irradiating waste with near-infrared, ultraviolet, or x-ray wavelengths for quantification can be done without dying waste beforehand. Nonetheless, textile-waste combinations were also needed to calibrate measurement systems. Irradiation also caused damage to textiles after prolonged exposure.[23, 24, 26, 27] A noninvasive measurement approach can be done with image analysis due to the periodic nature of textile structures and image converting algorithms. However, it is possible to undertrain algorithms with improper textile-sensor alignment and combination.[25, 26] Yet, in a practical sense, References 18-20 and 23-27's cleanliness quantification methods of a single article are not favorable because typical laundering consists of a bulk of textiles.

Observing waste transporting away from a textile bulk also serves as a viable quantification method, References 21, 28, and 29 outline ways to quantify the electrolytes and organic waste on a bulk of textiles. With a significant quantity of salt expected on textiles, conductivity sensors in wastewater provided a reliable reading on the mass transfer rates of salts and surfactants.[21] Reference 28 observed the air within an agitation chamber and noted that the ozone decomposition rate is proportional to the amount of organic waste within the chamber. Regardless of the model fit, ozone is consumable, leaves a residual smell on textiles, does not clean textiles, and does not interact with non-organic molecules. Reference 29 found that off-the-shelf technology could quantify small concentrations of cortisol and amine biomarkers (common human-produced biomarkers) in a saline solution (wastewater) with an ultraviolet spectrometer without preparing the sample for analysis. Although a linear relationship between concentration and absorbance was determined, there was no mention of the sample flowing through the optical path. Moreover, Reference 29's method would incorporate the abundance of particulates and microbes. Similar to References 23 -27, References 28 and 29 also did not attempt to quantify waste removal while laundering.

In closing, there are many methods to quantify the cleanliness of textiles after laundering, with some methods providing more practical applications. For example, References 23-27 provided high-accuracy methods at the expense

of labor and textile damage, while References 21, 28, and 29 generalized the quantification from measuring the waste transport out of textiles. Overall, conductivity measurement combined with wastewater observation may provide the best solution in modeling and quantifying textile bulk cleanliness during a laundering process. Still, the spaceflight environment may further limit cleanliness quantification sensing and modeling.

3. Utilizing Human Power in Spaceflight

Laundering textiles on Earth started with humans exerting power, and off-Earth laundering can take a similar approach. Frequent exercise is required off-Earth; References 30 through 33 review the design of off-Earth exercise machines and their ability to keep humans healthy. Lastly, Refs. 1 and 10 through 17 are reviewed with Ref. 30 through 32 in the context of applicable spaceflight engineering and operations principles. The synthesis of off-Earth exercise and textile laundering apparatus offers a preliminary solution to spaceflight laundering with human power in alternating gravity fields.

Currently, there are many spaceflight exercise machines in use and development. Reference 30 evaluates the International Space Station's (ISS) Advanced Resistive Exercise Device (ARED), while References 31 and 32 explore compact pully driven exercise machines. Although the ARED can exercise 20 different muscle groups and provide a two-point skeletal loading, it is far too large and power-consuming for current exploration vehicles and does not have an aerobic exercise component.[30] Reference 31 evaluates a similar two-point skeletal loading system with a resistive bar attached to pullies; likewise, there is no aerobic capability. Reference 32's Miniature Exercise Device - 2 is a compact motor and pully device for aerobic and resistive exercise capable of getting the user to achieve a maximum heart rate for an extended period; however, the resistive component cannot effectively load skeletons. Regardless of the mechanism, the context of spaceflight dictates the hardware needed to capture and convert human power.

A general spaceflight exercise hardware framework emerges from References 1, 10-17, 30-32. Due to the critical health risks from atrophy, exercise machines must have robust, simple, and serviceable designs. From the user's perspective, the interface and machine operation should be intuitive. The exercise motion envelope and machine stowage volume should be as minimal as possible, and vibration isolation systems may be needed.[1,10-17,30-32] Each topic mentioned thus far in capturing human power sets a context to design and evaluate a human-powered spaceflight textile laundering machine. However, none of the reviewed articles mention converting human power in spaceflight into hydraulic and electrical power.

C. Literature Review Conclusion

All considered, a combined exercise and textile laundering machine to improve human health in space is possible in the context of current research. Compared to domestic machine agitation methods, high-frequency fiber flexing improves waste transfer off textiles and reduces textile damage, and clean water rinsing also promotes a high rate of waste transfer; however, humans are quickly satisfied with textile cleanliness regardless of optimal laundering configurations.[18-29] A minimal resource consumption solution to quantify cleanliness uses conductivity sensors and an appropriate wavelength spectrometer to analyze textile wastewater in real time until an equilibrium state is reached.[23-29] Lastly, in spaceflight, the simultaneous working out and laundering should conserve astronaut time within a twenty-four-hour period, and the device performs two health risk reduction activities within a small volume that can travel with an astronaut wherever they go.[1,10-17,30] Without a precedent to compare, a preliminary design solution and method are needed to launder textiles off-Earth with human power.

III. Proposed Solution

Designing a spaceflight exercise and textile laundering machine requires evaluation of the *Literature Review*, insight into determining engineering design requirements, and forethought of how the machine will be treated throughout its lifetime. The machine presented and evaluated in this paper does not address the detergent aspect of laundry due to the complexity and heritage of laundry chemistry. What follows are initial design decisions and conceptual layout (Figures 1 and 2) for a preliminary spaceflight exercise and textile laundering machine to improve human health, which will be evaluated with Bond Graph Theory later in the paper.

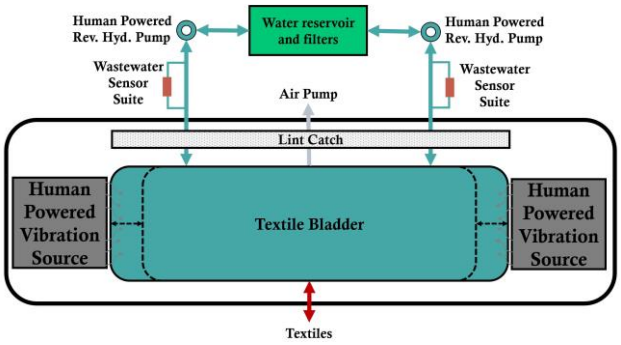

Figure 1. Spaceflight exercise and textile laundering machine concept diagram.

A. Textile and Waste Combination

Specific textile-waste combinations play an essential role in determining a laundering process. The prototype machine will evaluate cotton-based exercise textiles (>80% cotton with polyester and spandex) because they are abundant, familiar, and damage-prone. Synthetic perspiration will replicate the ample amounts of perspiration per individual deposited onto textiles.

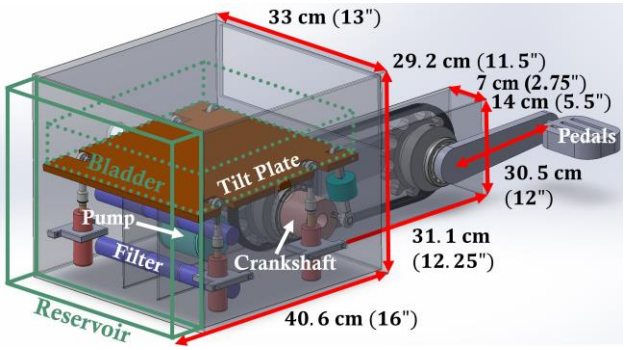

Figure 2. Annotated spaceflight exercise and textile laundering machine concept layout.

B. Humans Input Power

Astronauts exercise for prolonged periods each twenty-four-hour cycle, depositing large quantities of perspiration on textiles. A machine that simultaneously acts as an exercise and laundering machine will conserve crew time, counter human atrophy, and mitigate the risk of exposure to biohazard-ridden textiles. A robust and straightforward exercise machine can be designed around pedals. Arms or legs could power the mechanism, and simple off-the-shelf devices can convert rotary motion into translational motion, electrical potentials, and hydraulic pressure differentials.

C. Closed-Loop Water System

Due to the limited access to water off-Earth, laundering textiles during spaceflight should conserve and reuse the laundering water. A closed-loop water flow path with reservoirs and filters can mitigate water usage over time. The reservoir acts as a liquid capacitor that can set hydraulic pressure and be refilled. The filters aim to remove proteins, hydrocarbons, microbes, ionic species, and particulates from the water to generate favorable concentration gradients. Although detergents and other surfactants will be present in laundry, designing and evaluating a corresponding filter is outside the scope of this paper. However, through spaceflight engineering practices, the filters presented in this paper can be serviced or replaced in the future to address detergents and surfactants.

D. Vibration Agitation Bladder

Controlling fluids in microgravity is not trivial, so wetting and wringing textiles in microgravity may also not be trivial. In our proposed design, a flow-through flexible bladder ensures that all textiles are submerged in water before laundering. A flexible bladder can be filled with water and textiles simultaneously, even if the volume of textiles changes. A flexible bladder can also compress the textiles within to wring out wastewater towards an exit area of the bladder while vibrating to promote further water release. In addition, the ability for water to flow through the bladder may produce favorable waste concentration gradients between the textile and water. The bladder is mounted on a human-powered tilt plate mechanism (Figure 4) that users can adjust to meet exercise and laundering needs. Although the plate cannot achieve the same frequencies as ultrasonic baths, the vibration agitation laundering method shows potential in promoting the removal of organic, particulate, and oily substances with less detergent and reducing textile abrasion compared to traditional domestic Earth laundering machines.

E. Diode Spectrometer Analysis

Quantifying the abundance of organic and non-organic waste on textiles is typically limited to a labor-intensive post-laundering analysis of a single textile article. However, in the context of mass transfer, all the waste removed from textiles must enter the washing water, which means that quantifying waste in the water informs how clean a bulk of textiles are becoming during a laundering process. Knowing that human-produced organic waste is typically highly water soluble and contains primary amine groups, an appropriate wavelength can be selected for wastewater spectroscopy. Off-the-shelf primary amine diode spectrometers consist of a single wavelength Light-emitting Diode (LED) at 275 nm, a photon detector operating in the 240-360 nm range, milliamp electronics, and microliter flow cells. The Beer-Lambert Law can then quantify the abundance of particulates (e.g., dead skin, lint, and regolith) and primary amine groups (e.g., perspiration, sebum, and microbes) by knowing the LED emission intensity and calculating the detected intensity on the other side of the flow cell.

Lenses and windows are used to focus the emitted photons through the water and onto the sensor detection area by enabling Ultraviolet-B (250 nm) through visible light (700 nm) wavelength photons to pass through. The housing includes dark chambers to reduce outside photon interference and electronic protection from water. Again, through spaceflight engineering practices, the specific LED and photon detector wavelengths presented in this paper can be serviced and replaced in the future to address other wastewater spectroscopy needs.

F. Stand Alone

Current lunar exploration plans outline the different spacecraft and habitats humans will live in while traveling to and from the Moon. In addition, there are multiple LEO space stations under development for tourism. However, each spacecraft, space habitat, and space station have unique habitable volumes, Environmental Control and Life Support Systems, and available resources during a mission. Therefore, an initial laundering machine for spaceflight should be a standalone machine to reduce design complexity, ensure nominal operation regardless of habitable volume, and enable easy transport of the machine between different spacecraft, space habitats, and space stations. In addition, because the machine travels with humans during their spaceflight experience, it needs to operate in Earth's, the Moon's, and microgravity without significant alterations, regardless of workout regimen or input power source changes.

IV. Methods

The device concept takes human power as an input and converts the power into chemical concentration gradients and mechanical, electrical, and hydraulic power to launder textiles. This paper utilizes Bond Graph Theory to simulate the device's coupled mechanical, electrical, hydraulic, and chemical properties to inform concurrent device design and hardware selection to mature the technology to an appropriate technology readiness level. Understanding how humans power and configure the device is essential to predicting the overall waste removal rate of textiles. From hardware acquisition, device manufacturing, and sensor data collection, the Bond Graph model can be adjusted and verified to produce accurate waste removal rate data.

A. Bond Graph Theory Basics

Bond Graph (BG) modeling is a graphical method built from the first principles of energy conservation that shows the flow of information and energy within real and arbitrary parts of a system.[33] Energy flow modeled with linear and nonlinear differential and algebraic equations can be solved with computer code to obtain time and frequency domain responses. The BG technique produces a topological graph that uses interconnected elements to generate the system's codable first-order differential state space. Furthermore, the BG method reduces the time needed to derive entire sets of equations for a dynamic or static system while producing symbolic and numeric transfer functions for *concurrent* controller and hardware design and selection.

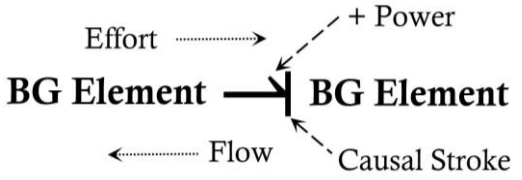

Figure 3. Bond Graph Power Bond structure.

Only a few BG symbols model entire systems; each symbol interacts with power. Traditional BG power is composed of two conjugate variables defined by the International System of Units, an effort (across variable) and a flow (through variable) where the product of the variables has the units of power in Watts. The most common symbol, a *power bond*, and its components are shown in Figure 3. The horizontal line joins two elements, the arrowhead indicates the direction of positive power, and the vertical line indicates a *causal stroke* or direction of the effort signal. Causality cannot be assigned to power bonds until the entire system is modeled and simplified because equations are derived depending on the corresponding element's *constitutive relation* (Φ).

A BG element's constitutive relation, or mathematical model, are functions of an inputted effort or flow, a generalized momentum (integral of effort), and or displacement (integral of flow) state variable. Table 1 summarizes the different state variables used in this paper. BG elements are ideal and are either a power source, dissipator, conserver, converter, or junction. Ten additional BG elements are summarized in Table 2. Regardless of causality, models oscillate when inertia and compliance elements interact, motion decays occur when inertia and resistance elements interact, and energy dissipation occurs rapidly when compliance and resistance elements interact.[33]

Effort and flow source elements have one permissible causality because they enforce an effort or flow. Compliance and inertia elements utilize displacement and momentum variables in an integral or derivative causality. It is generally preferred if compliance and inertial elements are in integral causality. Because of power conservation and enforced relationships, the transducers and gyrators have two causality configurations. Zero-junctions may only have one causal stroke nearest the junction to enforce the common effort. One-junctions may only have one causal stroke away from the junction to enforce the common flow. A simulation can be coded with system diagrams, element constitutive relations, a causally correct BG, and an ordinary differential equation solver.

Things to consider while developing BGs are that oversimplifying models may lead to poor results, no model can be exactly like a real system, it is the modelers' discretion to assign signs and determine how much system detail is required, and lastly, the initial state of the system and future time history of the input signal must be known. The construction, simplification, and use of multiple energy domain BG models require further explanation, reading, derivation, and examples outside this paper's scope but can be found in References 33 through 38, 40, and 41.

Table 1: Bond Graph Power Domain State Variables				
Domain	**Effort (e)**	**Flow (f)**	**Momentum (p)**	**Displacement (q)**
Mechanical Translation	Force (N)	Velocity $\left(\frac{m}{s}\right)$	Momentum $(N \cdot s)$	Displacement (m)
Mechanical Rotation	Torque $(N \cdot m)$	Angular Velocity $\left(\frac{rad}{s}\right)$	Angular Momentum $(N \cdot m \cdot s)$	Angle (Rad)
Electrical	Voltage (V)	Current (A)	Flux Linkage $(V \cdot s)$	Charge (C)
Hydraulic	Pressure $\left(\frac{N}{m^2}\right)$	Volumetric Flow Rate $\left(\frac{m^3}{s}\right)$	Pressure Momentum $\left(\frac{N \cdot s}{m^2}\right)$	Volume (m^3)
Chemical	Chemical Potential $\left(\frac{J}{mol}\right)$	Molar Flow $\left(\frac{mol}{s}\right)$	-	Molar Mass (mol)

Table 2: Common Bond Graph Elements			
Element	**Symbol**	**Description**	**Math Relationships**
Effort Source	S_e	Enforces effort value over time	$e(t) = E(t)$
Flow Source	S_f	Enforces flow value over time	$f(t) = F(t)$
Resistor	R	Power dissipating	$e = \Phi_R(f)$ f= $\Phi_R^{-1}(e)$
Compliance	C	Power storing	$e = \Phi_C^{-1}\left(\int^t f dt\right)$ f= $\frac{d}{dt}\Phi_C(e)$
Inertia	I	Power storing	$f = \Phi_I^{-1}\left(\int^t e dt\right)$ e= $\frac{d}{dt}\Phi_I(f)$
Transformer	TF	Power conservation	$me_1 = e_2$, $f_1 = mf_2$
Gyrator	GY	Power conservation	$re_1 = f_2$, $f_1 = re_2$
Zero-Junction	0	Common effort junction	$\sum f_i = 0$
One-Junction	1	Common flow junction	$\sum e_i = 0$
Active Bond	Information bond with zero power consumption.		

B. Mechanical Domain

Assuming humans can power a crankshaft with arms or legs, many translational and rotational mechanical devices can be powered. The primary mechanism for the current design is the agitation plate. The plate must impart oscillatory momentum of at least 2 Hertz onto textiles submerged in water.[21] Although a shaker plate or linear actuator can produce higher frequency vibrations, the hydraulic connection points would experience more mechanical fatigue than a rotating connection point at the hinge. It is also assumed that more deformation of the agitation bladder causes higher waste removal by imparting a load gradient across the textiles. A tilting plate mechanism can impart momentum in two orthogonal directions; if water flows through the textiles in another orthogonal direction, water momentum is imparted on the textiles in three principal axes - Figure 4 shows a diagram of such a mechanism. Figure 5 shows a tilt plate mechanism BG with elements that have linear constitutive relations. Note that the inertia of the tilt plate $\left(I: J_{tp}\right)$ depends on the volume of water in the bladder capacitor element.

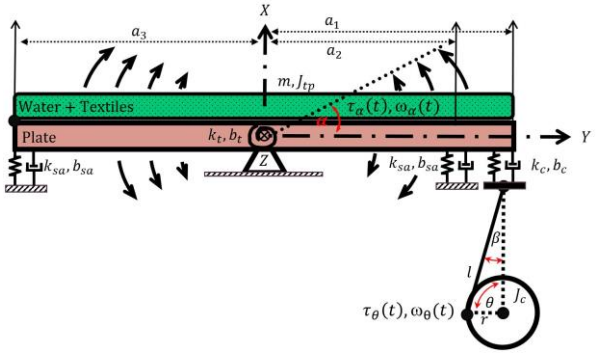

Figure 4. Tilt plate mechanism concept.

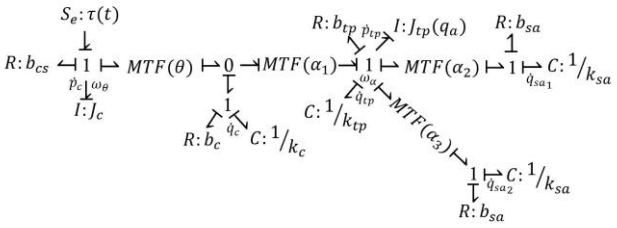

Figure 5. Bond Graph of tilt plate mechanism concept.

C. Electrical Domain

The crankshaft may also be attached to a permanent magnet generator to power the electrical system outlined in Figure 6. However, evaluating the electrical schematic reveals that a minimum of 270 mA is required to power the entire electrical system. With a minimum flow requirement, it is not of significant impact if power-conserving elements are neglected. Instead, only the resistive effects of the electronics will be considered in the construction of the electrical BG in Figure 7 at this time.

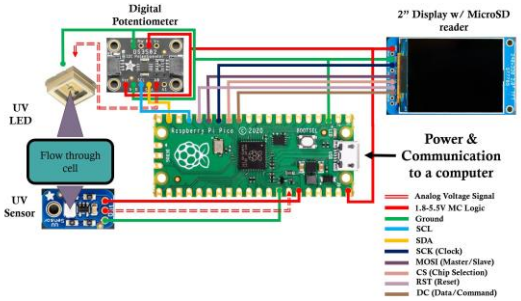

Figure 6. Electrical system concept.

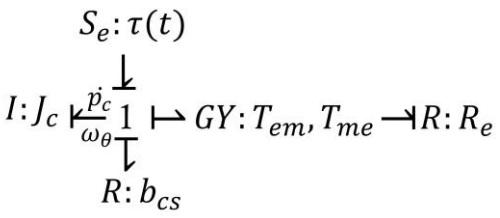

Figure 7. Bond Graph of electrical system concept.

D. Hydraulic Domain

The crankshaft may also be attached to a reversible hydraulic pump to power the system outlined in Figure 8. Hydraulic valves, porous plugs, and small passageways in the hydraulic system are modeled as energy-dissipating BG elements. Modified Ergun Equations can be used as constitutive relations to determine the pressure drop across the porous plugs as a function of a uniform volumetric flow rate.[39] The water filters can be modeled as a porous plug with a spherical particle bed and the lint catch with cylindrical fibers. It is generally difficult to model or predict the resistive functions and coefficients without pressure and volumetric flow rate measurements. Therefore, the water filters and lint catches of Figure 8 can be modeled as linear porous plug resistors in Figure 9 to reduce model complexity initially. The flexible agitation bladder that holds the textiles is a compliant BG element driven by the ratio of textiles to water in the bladder. Assuming the bladder is a thin-walled pressure vessel, the stress and strain relationship in the thin-walls can relate the bladder's volume change to the pressure change.[33] The flexible water reservoir and filters can also act as a compliance BG element. The BG model reveals a parallel variable resistor structure, which aligns well with meeting user needs regardless of torque direction. Some needs include a reservoir and water filter loop to clean the washing fluid and an agitation bladder and water reservoir loop to fill and remove water from the agitation bladder. Furthermore, the valves can also be used to increase power feedback (exercise resistance).

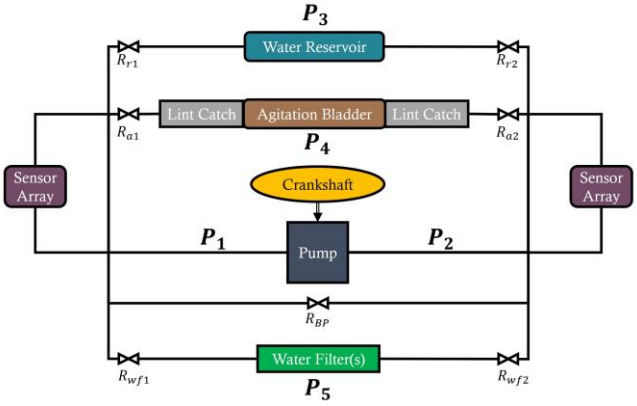

Figure 8. Hydraulic system concept.

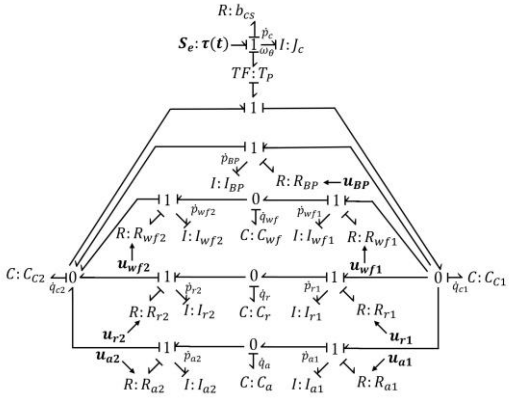

Figure 9. Bond Graph of hydraulic system concept.

E. Chemical Domain

In addition to the chemical domain information in Table 1, chemical BGs use absolute temperature and pressure as efforts and the time derivative of entropy and volume as flows.[37] The information in Table 1 is determined using Gibbs Free Energy functions and assuming constant pressure and temperature. Chemical BGs use scalar flow to conserve mass within the system, not moles of chemical species, which are used as transformer elements that interact with other BG elements. Furthermore, chemical processes and reactions couple solvent diffusion, electrolyte interactions, and hydrodynamic dispersion, resulting in very complex BGs outside the scope of this paper.[37] For this paper, chemical BGs are used to determine the mass of waste dissolving into the water, with the textiles acting as a waste source and the filters acting as a waste sink. Figure 10 reports a basic diagram

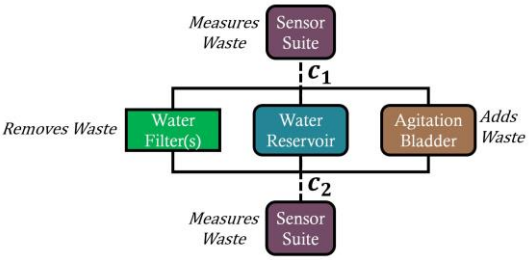

Figure 10. Chemical domain concept.

of the chemical domain. However, BG modeling issues arise when considering the state of a chemical process. Eventually, the reaction reaches equilibrium indicating that the resistor constitutive matrix Jacobian within the state space is symmetrical and the BG topology needs to change. Unfortunately, no tools or methods are available to reliability change BG model topology during a simulation.[33-38,40, 41] To overcome this modeling difficulty, Equation 1 can be derived to model the waste removal from textiles instead of using chemical domain constitutive relations.

Reference 6-8 uses a log-log relationship, Equation 1, to describe the amount of waste removed during laundering where $\bar{c}$ is the average concentration of waste removed, $\frac{\Delta c}{\Delta t}$ is the change in concentration over time, k is the waste removal rate coefficient normalized to $\frac{\Delta c}{\Delta t}$, and n is the kinetic order:

$$\bar{c} = \left(\frac{1}{k} \cdot \frac{\Delta c}{\Delta t}\right)^{\frac{1}{n}} \tag{1}$$

Although derived from domestic machine agitation, specific textile contamination methods, and specific textile-waste combinations, the general first-order kinetics equation still holds across other experiments.[6-8] The change in concentration over time $\left(\frac{\Delta c}{\Delta t}\right)$ can be calculated with the sensor suite. In general, the kinetic order (n) depends on the textile-soil combination, the agitation method, the amount of energy imparted on the textiles, how the textiles were contaminated, and the absorptivity of the textile. However, through various experiments, it was empirically found that the kinetic order ranges from 0.85 and 1.24.[6-8] Therefore, the range of the kinetic order will serve as generalized bounds for the estimated average amount of waste removed ($\bar{c}$).

The main uncertainty with this model is with the waste removal rate coefficient (k) because it is a function of time and the same factors as the kinetic order. Continual monitoring and calculating the waste removal rate may reduce the uncertainty during the laundering process; however, other time-dependent factors must be considered. Without chemical aids, the agitation method and power input significantly determine the waste removal rate coefficient.[6-8] Fundamentally, cleaning imparts momentum on waste to overcome binding forces; the vibration agitation plate and crossflow through the agitation bladder are the sources of momentum imparted on textile waste. Therefore, the vibration agitation plate and hydraulic system dynamics significantly affect the waste removal rate coefficient.

Another dependency of the waste removal rate coefficient is that the water flowing through the agitation bladder transports waste away from textiles, changing the waste concentration gradients near textiles and the probability of waste detaching from textiles. Lastly, the volume of textiles within the agitation bladder also affects the waste removal rate coefficient because the agitation bladder is of a relatively fixed volume and filled with water during all laundering cycles; therefore, with fewer textiles, there is more water interacting with the textiles to remove waste and vice versa.

An initial approach to combining all the factors affecting the waste removal rate coefficient is to calculate a single value in Hertz and then normalize the value to the change in concentration over time. First, three ratios are multiplied: the ratio of textile volume to agitation chamber volume, the ratio of water volume flux to agitation chamber volume in Hertz, and the ratio of mechanical momentum to hydraulic momentum interacting with textiles. The ratios identify how much energy is added to the textiles and the water before being scaled. The variables needed to calculate the waste removal rate coefficient are: the volume of the agitation chamber (V_A), the volume of textiles in the flow path (V_T), the volumetric flowrate of water through the agitation chamber ($\dot{q}_A$), the tilt plate momentum (p_{tp}), the water momentum in the agitation chamber (p_{a1}), and a scaling exponent (k_s) to account for textiles with various types of fabric, gravity effects, unknown time-and-rate dependent laundering processes, and the fusion of the data from the sensor suite.

$$k = \left[\left(\frac{\text{Textile Volume}}{\text{Chamber Volume}}\right)\left(\frac{\text{Water Volume Flux}}{\text{Chamber Volume}}\right)\left(\frac{\text{Mechanical Momentum}}{\text{Hydraulic Momentum}}\right)\right]^{k_s} = \left[\left(\frac{V_T}{V_A}\right)\left(\frac{\dot{q}_A}{V_A}\right)\left(\frac{|p_{tp}|}{|p_{a1}|}\right)\right]^{k_s} \tag{2}$$

Active bonds extend from corresponding mechanical and hydraulic BG elements to transmit the required information to compute Equations 1 and 2. The final mean soil removal value is the average of Equation 1 with an upper and lower kinetic order value. It is important to note that Equation 2 is specific to the laundering environment layout in this paper, and currently, there are no datasets to reinforce the derived model.

F. System Bond Graph

All the sub-subsections and information outlined in *Section IV* generate Figure 11, a BG of the exercise and textile laundering machine concept to relate human torque input to the rate of waste transported away from textiles in the agitation bladder. *Section V* outlines the simulation requirements and results of the BG model. Last, the constitutive relations are summarized in *Appendix* Table A1.

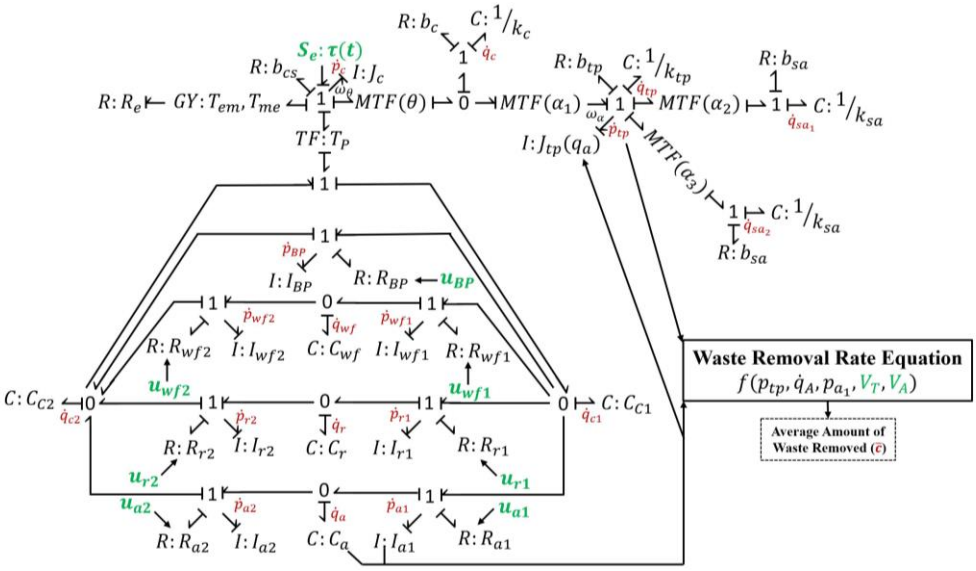

Figure 11. Bond Graph of Spaceflight exercise and textile laundering machine concept with inputs in green and outputs in red.

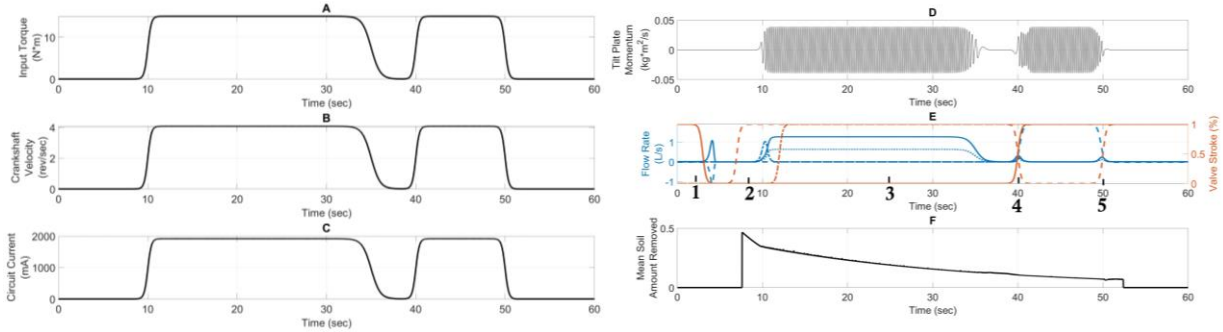

Figure 12. Bond Graph simulation results for an exercise and textile laundering machine concept. The phases of Subplot E - Phase 1 is the release of reservoir water (dashed blue) to fill the vacuum sealed agitation bladder (solid blue). Phase 2 is the closure of reservoir valves (dashed orange) and bypass value (dotted orange) as a torque signal is applied to the system at ten seconds. Phase 3 is the steady state operation of the machine under the applied torque signal. Phase 4 is the closure of water filter valves (dashed orange), opening of the reservoir valves (solid orange), and the closure of one agitation bladder value to draw water out of the textiles (dot-dash orange). Phase 5 is the closure of the open agitation bladder valve (dashed orange) and final ramp down and reconfiguration of the system for the next user.

V. Results and Analysis

MATLAB was used for the BG simulation, and the spaceflight exercise and textile laundering machine requires parameter values, a torque input, and the setting of the hydraulic valves. However, the first step in evaluating the results is to check the BG simulation model for Bounded Input Bounded Output (BIBO) stability, which was done with parameters that mimic real-world values and a sinusoid Heaviside step function approximation for both forward and backward pedaling acting on a variety of valve configurations. Six different valve configurations were used in testing: one with all flow paths open, one with all flow paths closed, and one with a single flow path open while the others are closed. Furthermore, the valve configurations were tested as initial conditions and then again as functions of time during a non-zero torque input. With a BIBO model, the machine performance indicators can be calculated: input torque in Newton meters, crankshaft speed in revolutions per second, electrical circuit current in milliamps, agitation plate angular momentum in Newton meter seconds, the flow rate of water in each flow path in liters per second with respect to value positions, and the mean soil concentration removed. Figure 12 reports a one-minute laundering process simulation as an example; note that the mean soil amount removed has been modified to the minute simulation instead of the empirically expected fifteen to twenty minutes. [6-8]

The torque input signal for this example was chosen as a series of Heaviside step approximations to better observe the system's behavior. In response to the input torque, the crankshaft accelerates to a constant and reasonable velocity of 4 revolutions per second, which varies slightly with different valve configurations. The simulated valve configurations are shown in subplot E in Figure 12.

Overall, the sequencing of valve actuation has a significant impact on crankshaft speed (power feedback), agitation chamber flow-through (water volume dynamics and cleaning ability), and water filtration (waste concentration control). The effect of valve configurations can also be seen on the generated electrical current (subplot C of Figure 12) and the plate angular momentum (subplot D of Figure 12); however, the plate angular momentum is more dependent on the flow rate through the agitation chamber which is also dependent on the valving configuration. The steady-state current is well above the lower limit of 270 mA, and the plate oscillates at about 3.5 Hertz. The valving configuration also dictates the flow rate of washing fluid through each hydraulic flow path. The flow rate through the agitation chamber and the water filters impacts the laundering process most; a high flow rate is desired for both. Phase 3 in subplot E of Figure 12 shows a desirable agitation chamber flow rate of around 1.25 liters per second and a water filter flow rate of around 0.6 liters per second. A coupling yet to be modeled is the water filter's cleaning effectiveness as a function of flow rate and its impact on the waste rate removal constant. Although the simulated sensed concentration decay rate is large for this example to show a significant change, the observed responses of the amount of waste removed from user torque and valving input show the potential to effectively meet the user's physical abilities, needs, and laundering desires.

VI. Concluding Discussion

This paper proposes a compact exercise and textile laundering machine that simultaneously addresses two activities in various gravity fields to reduce the stresses of off-Earth travel. Furthermore, the outlined approach to cleaning in space could also be extended to dishwashing, tool sanitization, and dust mitigation in lunar habitats. In the *Literature Review* context, a machine Bond Graph addresses the *Proposed Solution*. With these preliminary simulation results in hand, a preliminary mechanical system design is now in progress at UC Davis: Figure 13 shows a Computer-aided Design model of a section of the machine. The following subsections outline an approach to further the machine's technological maturity through key design parameters, sensor types and locations, and a general testing plan.

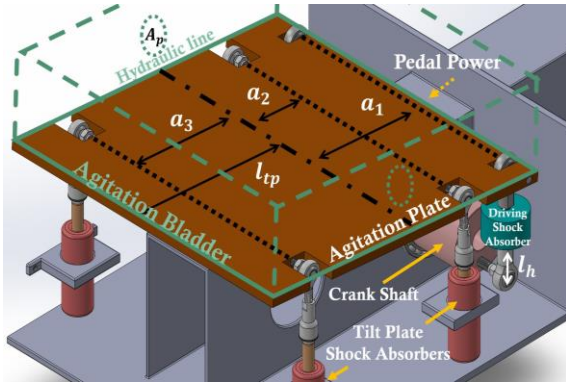

Figure 13. Computer-aided Design of the spaceflight exercise and textile laundering machine concept with a few components labeled.

A. Key Design Parameters

At a minimum, the machine should be able to wash a single exercise outfit (a pair of socks, a pair of shorts, a shirt, and undergarments) of a human in the 95th percentile for size in a single load. In addition, larger washing volumes should be considered to alleviate dirty laundry build-up from workout regimen deviations. Other machine aspects can be determined from the simulation parameters (Table 3) that have the most impact on the state variables, indicating the hardware that drives or limits the performance of each subsystem.

B. Sensors

The selection and placement of sensors in the system correspond to the energy domain under observation and the state variables present in a BG. The mechanical domain requires two sensors: an accelerometer on the edge of the agitation plate and an angular velocity sensor for the crankshaft. The hydraulic domain requires nine sensors - a flow meter near each valve and an absolute pressure transducer on each side of the hydraulic loop. The chemical domain sensors are selected to characterize the state of the wastewater. A diode spectrometer quantifies the abundance of organics and particulates in the water. A turbidity sensor measurement is a redundant particulate measurement of the diode spectrometer. Electrochemical sensors (amperometric, potentiometric, and voltammetric) observe electrolytes and other human-produced biomarkers. Furthermore, a thermometer, pH meter, and oxygen meter also determine the state of the wastewater. Although not all wastewater sensors are needed to quantify textile cleanliness, the information gathered from the sensor suite may enable the identification of specific health risks to astronauts before symptoms arise.[42] Further analysis of the wastewater sensors will inform the BG electrical domain modeling and what information should be presented to the user.

Table 3: Key Bond Graph Parameters			
Domain	**Parameter**	**Units**	**Design Consideration**
Mechanical	a_1	m	Distance between tilt plate hinge and driving shock absorber to tilt plate
	a_2	m	Distance between tilt plate hinge and shock absorber set #1 to tilt plate
	a_3	m	Distance between tilt plate hinge and shock absorber set #2 to tilt plate
	J_c	kg/m^2	Inertia of crankshaft
	l_{tp}	m	Length of tilt plate away from the rotation axis
	l_h	m	Crank arm length from crankshaft mount to crank arm shock absorber
	r	m	Distance from crankshaft axis of rotation to crank arm mount on crankshaft
Hydraulic	A_p	m^2	Area of hydraulic piping
	A_{lcp}	m^2	Area of lint catch porous plugs
	A_{wrp}	m^2	Area of water filter porous plugs
	V_A	m^3	Volume of agitation chamber bladder
	V_R	m^3	Volume of water reservoir bladder
	V_{wf}	m^3	Volume of water filter(s)

C. General Testing Plan

With informed hardware and sensor selection decisions, our space-laundry machine will be primarily manufactured with off-the-shelf components to reduce cost and increase robustness. As each subsystem nears completion, a testing and validation plan will be executed to ensure the subsystem meets the desired design and performance requirements. Testing of the spaceflight exercise and laundering machine will follow the energy domains. First, the mechanical agitation system is tested to evaluate vibration performance, human interaction, and hydraulic system interaction. Second, the hydraulic system tests evaluate flow rate performance, valve layout, and interaction with the wastewater observation system. Third, the wastewater observation system tests evaluate signal-to-noise performance, power consumption, and interaction with the electrical system. Fourth, BG model updating to match collected data. Last, an iterative process to test, modify and evaluate the entire system.

Once each subsystem completes manufacturing, testing, and validation, the machine will be assembled, tested, and validated. Data will be collected on Earth during testing and validation to further modify the Bond Graph model and mature the device from a Technology Readiness Level (TRL) of three up to five.[43] During the maturing process, it can be expected that hardware will be redesigned and replaced, redundant systems will be added to ensure proper performance during an anomaly, and additional design requirements will be introduced to comply with the spaceflight environment. After ground validation, microgravity validation on NASA-sponsored parabolic flights will be needed to mature the device up to a TRL of seven with the same process used to mature the device from three up to five.[44] Once a TRL of seven is achieved, designing, testing, and validating a flight-qualified machine begins.

Appendix

Table A1: Bond Graph Constitutive Relations					
Physical Element	**BG Element**	**Constitutive Relation**	**Physical Element**	**BG Element**	**Constitutive Relation**
Applied Torque	Effort Source	$S_{e_1} = \tau(t)$	Crank-Follower	Modulated Transformer	$m_1(\theta) = r\sin\theta + \frac{l\left(\frac{r}{l}\right)^2 \cos\theta \sin\theta}{\sqrt{1-\left(\frac{r}{l}\right)^2 \sin^2\theta}}$
Crankshaft	Inertia	$\Phi_{I_1} = J_C$	DC Generator	Gyrator	$r_1 = T_{em}$
Crankshaft Friction	Resistor	$\Phi_{R_1} = b_{cs}$	DC Generator	Gyrator	$r_2 = T_{me}$
Shock Abs. #1	Resistor	$\Phi_{R_2} = b_C$	Resistor	Resistor	$\Phi_{R_6}^{-1} = R_e$
Shock Abs. #1	Capacitor	$\Phi_{C_1} = \frac{1}{k_C}$	Hydraulic Pump	Transformer	$m_5 = T_P$
Hinge	Resistor	$\Phi_{R_3} = b_{tp}$	Path Inertia	Inertia	$\Phi_{I_{3_i}} = \frac{\rho l_i}{4 * A_i}$
Hinge	Capacitor	$\Phi_{C_2} = \frac{1}{k_{tp}}$	Hydraulic Valve	Resistor	$\Phi_{R_7} = \frac{\rho \Delta Q_i \lvert \Delta Q_i \rvert}{2C_d^2(u_i)A^2(u_i)}$
Tilt Plate	Inertia	$\Phi_{I_2} = J_{tp} + \frac{\rho q_a l_{tp}}{12}$	Lint Catch	Nonlinear Resistor	$\Phi_{R_8} = \frac{9.375\Delta Q \mu L\left(\frac{4}{D_p}\right)^2 (1-\varepsilon)^2}{A_{lcp}\varepsilon^3} + \frac{0.4375\Delta Q^2 \rho L\left(\frac{4}{D_p}\right)(1-\varepsilon)}{A_{lcp}^2\varepsilon^3}$
Shock Abs. #2	Resistor	$\Phi_{R_4} = b_{sa1}$	Water Filter	Nonlinear Resistor	$\Phi_{R_9} = \frac{4.167\Delta Q \mu L\left(\frac{6}{D_p}\right)^2 (1-\varepsilon)^2}{A_{wrp}\varepsilon^3} + \frac{0.2917\Delta Q^2 \rho L\left(\frac{6}{D_p}\right)(1-\varepsilon)}{A_{wrp}^2\varepsilon^3}$
Shock Abs. #2	Capacitor	$\Phi_{C_3} = \frac{1}{k_{sa1}}$	Lint Catch	Resistor	$\Phi_{R_{10}} = R_{lc}\Delta Q$

Shock Abs. #3	Resistor	$\Phi_{R_5} = b_{sa2}$	Water Filter	Resistor	$\Phi_{R_{11}} = R_{wf}\Delta Q$
Shock Abs. #3	Capacitor	$\Phi_{C_4} = \frac{1}{k_{sa2}}$	Agitation Bladder	Capacitor	$\Phi_{C_5} = \frac{6r_A V_A}{t_A E} + \frac{V_A}{B}$
Shock Abs. #1 Mount	Modulated Transformer	$m_2(\alpha_1) = a_1 cos\alpha$	Water Reservoir	Capacitor	$\Phi_{C_6} = \frac{10r_R V_R}{t_R E} + \frac{V_R}{B}$
Shock Abs. #2 Mount	Modulated Transformer	$m_3(\alpha_2) = a_2 cos\alpha$	Water Filter	Capacitor	$\Phi_{C_7} = \frac{V_{wf}}{B}$
Shock Abs. #3 Mount	Modulated Transformer	$m_4(\alpha_3) = a_3 cos\alpha$	Pipe	Capacitor	$\Phi_{C_8} = \frac{V_p}{B}$

Acknowledgments

Thank you, Dr. Donald Margolis and Dr. Dean Karnopp from the UC Davis Department of Mechanical and Aerospace Engineering for their pioneering, expertise, guidance, and insight into Bond Graph Theory. Thank you, Dr. Donald Land from the UC Davis Department of Chemistry for advice on surfactants and experimental chemistry procedures. Thank you, Dr. Mark Sivik from the Procter & Gamble Company for insight on detergent research.

References

[1]Ewert, Michael, et al. "Clothes Cleaning Research for Space Exploration." *TTU DSpace Home*, 51st International Conference on Environmental Systems, 10 July 2022, https://ttu-ir.tdl.org/handle/2346/89851.

[2]Brooks, J.H., and J.R. McPhee. "The Effect of Machine Action on Soil Removal from Wool during Laundering." *Textile Research Journal*, vol. 37, no. 5, May 1967, pp. 371–376., https://doi.org/10.1177/004051756703700506.

[3]Bubl, Janet L. "Laundering Cotton Fabric." *Textile Research Journal*, vol. 40, no. 7, July 1970, pp. 637–643., https://doi.org/10.1177/004051757004000709.

[4]Morris, Mary Ann. ". Laundering Cotton Fabric." *Textile Research Journal*, vol. 40, no. 7, July 1970, pp. 644–649., https://doi.org/10.1177/004051757004000710.

[5]Huisman, Mary Ann, and Mary Ann Morris. "A Study of the Removal of Synthetic Sebum from Durable-Press Fabrics, Using a Liquid-Scintillation Technique." *Textile Research Journal*, vol. 41, no. 8, Aug. 1971, pp. 657–661., https://doi.org/10.1177/004051757104100804.

[6]Kissa, Erik. "Kinetics and Mechanisms of Detergency – Part I: Liquid Hydrophobic (Oily) Soils." *Textile Research Journal*, vol. 45, no. 10, Oct. 1975, pp. 736–741., https://doi.org/10.1177/004051757504501007.

[7]Kissa, Erik. "Kinetics and Mechanisms of Detergency - Part II: Particulate Soil." *Textile Research Journal*, vol. 48, no. 7, July 1978, pp. 395–399., https://doi.org/10.1177/004051757804800705.

[8]Kissa, Erik. "Kinetics and Mechanisms of Detergency – Part III: Effect of Soiling Conditions on Particulate Soil Detergency." *Textile Research Journal*, vol. 49, no. 7, July 1979, pp. 384–389., https://doi.org/10.1177/004051757904900703.

[9]Ganguli, K.L., and J. Van Eendenburg. "Mass Transfer in a Laboratory Washing Machine." *Textile Research Journal*, vol. 50, no. 7, July 1980, pp. 428–432., https://doi.org/10.1177/004051758005000707.

[10]Teichert, W., and M. Klein. "The Dynamic Behaviour of Fluids in Microgravity." *The Dynamic Behaviour of Fluids in Microgravity*, European Space AgencyF, Feb. 1996, https://www.esa.int/esapub/bulletin/bullet85/klein85.htm.

[11]Ploutz-Snyder, Lori. "Prevention of Muscle Atrophy with Exercise Countermeasures: Where We Are and Where We Are Going - NASA Technical Reports Server (NTRS)." *NASA*, NASA, 29 Jan. 2009, https://ntrs.nasa.gov/search.jsp?R=20090007465.

[12]Beyene, Nahon M. "Defining Exercise Performance Metrics for Flight Hardware Development - NASA Technical Reports Server (NTRS)." *NASA*, NASA, 1 Jan. 2004, https://ntrs.nasa.gov/citations/20060010440.

[13]LeBlanc, Adrian. "JSC Human Life Sciences Project - NASA Technical Reports Server (NTRS)." *NASA*, NASA, 1 Feb. 1998, https://ntrs.nasa.gov/citations/19980206468.

[14]Beyene, Nahom M. "The Art of Space Flight Exercise Hardware: Design and Implementation - NASA Technical Reports Server (NTRS)." *NASA*, NASA, 1 Jan. 2004, https://ntrs.nasa.gov/citations/20060023359.

[15]Rafalik, Kerrie K. "Crew Exercise - NASA Technical Reports Server (NTRS)." *NASA*, NASA, 5 Dec. 2017, https://ntrs.nasa.gov/citations/20170011663.

[16]Perusek, Gail, Lewandowski, Beth, Nall, Marsha, Norsk, Peter, Linnehan, Rick, and Baumann Davis. "Human Research Program Advanced Exercise Concepts (AEC) Overview - NASA Technical Reports Server (NTRS)." *NASA*, NASA, 10 Feb. 2015, https://ntrs.nasa.gov/search.jsp?R=20160012339.

[17]Toder, Carly, Gipson, Iona, Conley, Danielle, Nieschwitz, Linda, and Austin Perk. "Countermeasures (Ired, Ared CEVIS, MEC, Tvis, T2, Periodic Fitness Evaluation, BP-ECG, HRM). Critical Readiness Review Increment 23 and 24 - NASA Technical Reports Server (NTRS)." *NASA*, NASA, 4 Feb. 2010, https://ntrs.nasa.gov/citations/20100008451.

[18]Mercadé-Prieto, Ruben, and Serafim Bakalis. "Methodological Study on the Removal of Solid Oil and Fat Stains from Cotton Fabrics Using Abrasion." Textile Research Journal, vol. 84, no. 1, 2013, pp. 52–65., https://doi.org/10.1177/0040517513490059.

[19]Lee, Ahjin, Seo, Moon Hwo, Yang, Seungdo, Koh, Joonseok, and Hyungsup Kim. "The Effects of Mechanical Actions on Washing Efficiency." Fibers and Polymers, vol. 9, no. 1, 2008, pp. 101–106., https://doi.org/10.1007/s12221-008-0017-1.

[20]Shin, Sangwoo, Warren, Patrick B., and Howard A. Stone. "Cleaning by Surfactant Gradients: Particulate Removal from Porous Materials and the Significance of Rinsing in Laundry Detergency." Physical Review Applied, vol. 9, no. 3, 2018, https://doi.org/10.1103/physrevapplied.9.034012.

[21]Warmoeskerken, M.M.C.G, van der Vlist, P., Moholkar, V.S., and V.A Nierstrasz. "Laundry Process Intensification by Ultrasound." Colloids and Surfaces A: Physicochemical and Engineering Aspects, vol. 210, no. 2-3, 2002, pp. 277–285., https://doi.org/10.1016/s0927-7757(02)00372-2.

[22]Ma, Mingbo, You, Lizia, Chen, Lican, and Wenlong Zhou. "Effects of Ultrasonic Laundering on the Properties of Silk Fabrics." Textile Research Journal, vol. 84, no. 20, 2014, pp. 2166–2174., https://doi.org/10.1177/0040517514537370.

[23]Prato, H.H., and M.A. Morris. "Soil Remaining on Fabrics after Laundering as Evaluated by Response Surface Methodology." Textile Research Journal, vol. 54, no. 10, Oct. 1984, pp. 637–644., https://doi.org/10.1177/004051758405401001.

[24]Ghosh, Subhas, Cannon, Michael D., and R. B. Roy. "Quantitative Analysis of Durable Press Resin on Cotton Fabrics Using near-Infrared Reflectance Spectroscopy." Textile Research Journal, vol. 60, no. 3, Mar. 1990, pp. 167–172., https://doi.org/10.1177/004051759006000308.

[25]Kim, Soo Chang, Kang, Tae Jin, Hong, Kyung Hwa, and Bugao Xu. "Image Analysis for Quantifying Marquisette Damage in Home Laundering." Textile Research Journal, vol. 75, no. 6, June 2005, pp. 474–479., https://doi.org/10.1177/0040517505053868.

[26]Gururajan, Arunkumar, Hequet, Eric F., and Hamed Sari-Sarraf. "Objective Evaluation of Soil Release in Fabrics." Textile Research Journal, vol. 78, no. 9, 2008, pp. 782–795., https://doi.org/10.1177/0040517507090786.

[27]Sugita, Keiko, and Masaru Oya. "Improvement of the Image Analysis Method for Quantifying Low-Polarity Oily Stains on Fabric." Textile Research Journal, vol. 92, no. 5-6, 2021, pp. 649–659., https://doi.org/10.1177/00405175211041719.

[28]Krifa, Mourad, Rajaganesh, Shamini, and Willaim Fahy. "Perspectives on Textile Cleanliness – Detecting Human Sebum Residues on Worn Clothing." Textile Research Journal, vol. 89, no. 23-24, 2019, pp. 5226–5237., https://doi.org/10.1177/0040517519855323.

[29]Ray, Prajokta, and Andrew J. Steckl. "Label-Free Optical Detection of Multiple Biomarkers in Sweat, Plasma, Urine, and Saliva." ACS Sensors, vol. 4, no. 5, 2019, pp. 1346–1357., https://doi.org/10.1021/acssensors.9b00301.

[30]Raboin, Jasen, Niebuhr, Jason, Cruz, Santana, and Chris Lamoreaux. "Advanced Resistive Exercise DEVICE - NASA Technical Reports Server (NTRS)." NASA, NASA, 1 Oct. 2007, https://ntrs.nasa.gov/citations/20100011132.

[31]Downs, Meghan E. "Novel Musculoskeletal Loading and Assessment System - NASA Technical Reports Server (NTRS)." NASA, NASA, 23 Jan. 2017, https://ntrs.nasa.gov/search.jsp?R=20170000271.

[32]Maynard, Graig, Zumbado, Fernando, Newby, Nate, Humphreys, Bradley T., and Meghan E. Downs. "Miniature Exercise Device-2 (MED-2): Preliminary ISS Evaluation Results for a Compact Motorized Resistive and Aerobic Rowing Exercise Device-NASA Technical Reports Server (NTRS)." NASA, NASA, 23 July 2018, https://ntrs.nasa.gov/citations/20180006490.

[33]Karnopp, Dean, Margolis, Donald, and Ronald Rosenberg. System Dynamics: Modeling, Simulation and Control of Mechatronic Systems. Fifth ed., Wiley, 2012.

[34]Granda, Jose, and Raymond Montgomery. "Automated Modeling and Simulation Using the Bond Graph Method for the Aerospace Industry." *AIAA Modeling and Simulation Technologies Conference and Exhibit* 2003, https://doi.org/10.2514/6.2003-5527.

[35]Borutzky, W. "Bond Graph Modelling and Simulation of Multidisciplinary Systems – an Introduction." *Simulation Modelling Practice and Theory*, vol. 17, no. 1, 14 Sept. 2007, pp. 3–21., https://doi.org/10.1016/j.simpat.2007.08.008.

[36]Borutzky, Wolfgang. Bond Graphs for Modelling, Control and Fault Diagnosis of Engineering Systems. Springer International Publishing, 2018.

[37]Oster, George F., Perelson, Alan S., and Aharon Katchalsky. "Network Thermodynamics: Dynamic Modelling of Biophysical Systems." Quarterly Reviews of Biophysics, vol. 6, no. 1, 1973, pp. 1–134., https://doi.org/10.1017/s0033583500000081.

[38]Broenink, J. "Introduction to Physical Systems Modelling with Bond Graphs." *Introduction to Physical Systems Modelling with Bond Graphs*, 1 Jan. 2000, https://www.semanticscholar.org/paper/Introduction-to-Physical-Systems-Modelling-with-Broenink/edbe4223c787adebd6e4674317a197312ecef87d.

[39]Krotiuk, William J. Calculation of Pressure Drop across a Porous Media Debris Bed on a PWR ... U.S. Nuclear Regulatory Commission / Office of Nuclear Regulatory Research, 12 Nov. 2006, https://www.nrc.gov/docs/ML0632/ML063210166.pdf.

[40]Karnopp, Dean. "Bond Graph Models for Electrochemical Energy Storage: Electrical, Chemical and Thermal Effects." Journal of the Franklin Institute, vol. 327, no. 6, 1990, pp. 983–992., https://doi.org/10.1016/0016-0032(90)90073-r.

[41]Selişteanu, Dan, Roman, Monica, and Dorin Şendrescu. "Pseudo Bond Graph Modelling and on-Line Estimation of Unknown Kinetics for a Wastewater Biodegradation Process." Simulation Modelling Practice and Theory, vol. 18, no. 9, 2010, pp. 1297–1313., https://doi.org/10.1016/j.simpat.2010.05.004.

[42]Sempionatto, Juliane R., Lasalde-Ramerírez, José A., Mahato, Kuldeep, Wang, Joseph, and Wie Gao. "Wearable Chemical Sensors for Biomarker Discovery in the Omics Era." *Nature Reviews Chemistry*, vol. 6, no. 12, 15 Nov. 2022, pp. 899–915., https://doi.org/10.1038/s41570-022-00439-w.

[43]Dunbar, Brian. "Technology Readiness Level." NASA, NASA, 6 May 2015, https://www.nasa.gov/directorates/heo/scan/engineering/technology/technology_readiness_level.

[44]Newton, Laura. "Accessing Flight Tests." NASA, NASA, 7 Sept. 2021, https://www.nasa.gov/directorates/spacetech/flightopportunities/opportunities#Solicitation.